Materials Science-Poland, 35(4), 2017, pp. 806-815
http://www.materialsscience.pwr.wroc.pl/
DOI: 10.1515/msp-2017-0105

DE GRUYTER OPEN

Microstructure and dielectric properties of La_2O_3 doped Ti-rich barium strontium titanate ceramics for capacitor applications

CHEN ZHANG[1,*], FANGXU CHEN[1], ZHIXIN LING[1], GANG JIAN[1], YUANLIANG LI[2]

[1]Provincial Key Lab of Advanced Welding Technology, Jiangsu University of Science and Technology, Zhenjiang 212003, China

[2]Hebei Provincial Key Laboratory of Inorganic Nonmetallic Materials, North China University of Science and Technology, Tangshan 063009, China

Microstructure and dielectric properties of La_2O_3 doped Ti-rich barium strontium titanate ceramics, prepared by solid state method, were investigated with non-stoichiometric level and various La_2O_3 content, using XRD, SEM and LCR measuring system. With an increase of non-stoichiometric level, the unit cell volumes of perovskite lattices for the single phase Ti-rich barium strontium titanate ceramics increased due to the decreasing A site vacancy concentration V''_A. The unit cell volume increased and then decreased slightly with the increasing La_2O_3 content. Relatively high non-stoichiometric level and high La_2O_3 content in Ti-rich barium strontium titanate ceramics contributed to the decreased average grain size as well as fine grain size distribution, which correspondingly improved the temperature stability of the relative dielectric constant. The relative dielectric constant ϵ_{rRT}, dielectric loss $\tan\delta_{RT}$ and the maximum relative dielectric constant ϵ_{rmax} decreased and then increased with the increasing non-stoichiometric level. With the increase of La_2O_3 doping content, the relative dielectric constant ϵ_{rRT} increased initially and then decreased. The maximum relative dielectric constant ϵ_{rmax} can be increased by applying low doping content of La_2O_3 in Ti-rich barium strontium titanate ceramics due to the increased spontaneous polarization.

Keywords: *barium strontium titanate; dielectric properties; point defects; perovskite*

1. Introduction

Barium titanate $BaTiO_3$ (BT) is a typical ABO_3 perovskite structure material [1] well-known for its excellent electric properties, which allow for its utilization in a variety of electronic applications such as multilayer capacitors, positive temperature coefficient resistors, transducers and so on [2–4]. The high relative permittivity and low dielectric loss of the material are favored in the microelectronics industry since they enable device miniaturization. Barium strontium titanate $Ba_xSr_{1-x}TiO_3$ (BST) is a solid solution family composed of barium titanate and strontium titanate with the Curie temperature covering a wide range from −250 °C to 120 °C. $BaTiO_3$ can transform upon temperature through the cubic paraelectric, ferroelectric tetragonal, orthorhombic and rhombohedral phase in descending order [5, 6]. When strontium atoms are introduced into A site in a perovskite barium titanate matrix to replace barium atoms, the phase transition temperature from paraelectric to ferroelectric decreases and the phase transition behavior changes from sharp to diffuse, which makes the temperature stability of dielectric parameters of BST ceramics better than that of BT ceramics in the phase transition temperature range [7]. However, in order to enable the BST ceramics to become a candidate for temperature stable "X7R" capacitor, one of the multilayer ceramic capacitor categories based on the standards of Electronic Industries Association (EIA) [8], the conflict between the excellent dielectric properties at room temperature and good dielectric temperature stability in the uniform BST ceramics [9] has to be overcome.

In the past decade, an effective process of introducing dopants of rare earth elements into BST at

*E-mail: czhang1981@hotmail.com

A and/or B site, was used rather than controlling Ba/Sr ratio to modify the BST dielectric properties [10–13]. The rare-earth element is found to be an effective factor in controlling the temperature-dependence of the dielectric properties. Doping a large rare-earth ion, such as La^{3+}, into the stoichiometric BST lattice results in the strong broadening of the Curie peak [14]. In our previous work, we have found that with the increase of La_2O_3 doping content, the dielectric constant and dielectric loss at room temperature for the stoichiometric $(Ba_{0.74}Sr_{0.26})TiO_3$ ceramics increase considerably [15].

It is well known that the dielectric properties of $BaTiO_3$ ceramics are not only dependent on the oxygen partial pressure (pO_2) and sintering temperature/time but also the overall A/B ratio [16]. Recently, some influences of A/B ratio on the microstructures and dielectric properties in BST ceramics have been gradually explained. Dong et al. [9] concluded that adding excessive TiO_2 could remarkably inhibit grain growth, as well as suppress and broaden the Curie peaks in compositionally inhomogeneous BST ceramics.

The above two methods, helping broaden the BST Curie peak, evoke our interests in the dielectric properties of rare earth element doped non-stoichiometric BST ceramics aiming for "Y5V" or "X7R" capacitor applications. Therefore, in this article we report a systematic study of the microstructure, point defect behavior and dielectric properties of Ti-rich $(Ba_{0.75}Sr_{0.25})Ti_{1+\delta}O_{3+2\delta}$ ceramics (A/B ratio <1) taking the trivalent La^{3+} ions as a dopant. The influences of δ value (namely the non-stoichiometric level) and La_2O_3 doping content on the point defect behavior and the dielectric properties of barium strontium titanate ceramics are discussed.

2. Experimental

Chemical compositions of the La_2O_3 doped Ti-rich barium strontium titanate specimens are given by the formula $(Ba_{0.75}Sr_{0.25})Ti_{1+\delta}O_{3+2\delta}$ + x wt.% La_2O_3 + 1.0 wt.% Sb_2O_3 (δ = 0, 0.002, 0.004, 0.006, 0.008; x = 0, 0.4, 0.8, 1.2, 1.6). The sample number for each chemical composition is shown in Table 1. High purity $BaCO_3$ (>99.0 %), $SrCO_3$ (>99.0 %), TiO_2 (>98.0 %) powders used as starting raw materials were weighed according to the above formulas, ball-milled for 14 h, dried and calcined at 1080 °C for 2 h. The calcined powders were mixed with La_2O_3 (> 99.99 %) and Sb_2O_3 (> 99.0 %), reground, dried and added with 5 wt.% polyvinyl alcohol (PVA) as a binder for granulation. The mixture was sieved through 60-mesh screen and then pressed into pellets, 10 mm in diameter and 2 mm in thickness under 250 MPa pressure. Sintering was conducted in air at temperatures between 1300 °C and 1330 °C for 1 to 4 h. For dielectric measurements, both flat surfaces of the specimens were coated with BQ-5311 silver paste after ultrasonic bath cleaning and then fired at 800 °C for 10 min.

The crystal structures of the specimens were studied by X-ray diffraction analysis (XRD, Rigaku D/max 2500v/pc) with CuKα radiation. The surface morphologies of the specimens were observed using the SEM (JSM-6480 ESEM). The capacitance value, electrical resistance R and dissipation factor D were measured with LCR-8101G Automatic LCR Meter at 1 kHz. The relative dielectric constant ϵ_r , the loss tangent tanδ and DC resistivity ρ were calculated as follows:

$$\varepsilon_r = \frac{1.44 \times 10^{11} Ch}{\Phi^2} \tag{1}$$

$$\tan\delta = D \tag{2}$$

$$\rho = \frac{\pi R \Phi^2}{4h} \tag{3}$$

where C is the capacitance value [F], h is the thickness [m], Φ is the diameter of the electrode [m] and R is the DC resistance [Ω]. An automatic measuring system consisting of an automatic LCR meter and THP-F-100 temperature control unit was used to record the temperature dependence of dielectric parameters in the temperature range of 20 °C to 50 °C at 1 kHz.

Table 1. Chemical compositions of the specimens.

Sample No.	δ	x	Composition
A0	0.000	0	$(Ba_{0.75}Sr_{0.25})TiO_3$ + 1.0 wt.% Sb_2O_3
A1	0.002	0	$(Ba_{0.75}Sr_{0.25})Ti_{1.002}O_{3.004}$ + 1.0 wt.% Sb_2O_3
A2	0.004	0	$(Ba_{0.75}Sr_{0.25})Ti_{1.004}O_{3.008}$ + 1.0 wt.% Sb_2O_3
A3/B0	0.006	0	$(Ba_{0.75}Sr_{0.25})Ti_{1.006}O_{3.012}$ + 1.0 wt.% Sb_2O_3
A4	0.008	0	$(Ba_{0.75}Sr_{0.25})Ti_{1.008}O_{3.016}$ + 1.0 wt.% Sb_2O_3
B1	0.006	0.4	$(Ba_{0.75}Sr_{0.25})Ti_{1.006}O_{3.012}$ + 0.4 wt.% La_2O_3+1.0wt.% Sb_2O_3
B2	0.006	0.8	$(Ba_{0.75}Sr_{0.25})Ti_{1.006}O_{3.012}$ + 0.8 wt.% La_2O_3 + 1.0 wt.% Sb_2O_3
B3	0.006	1.2	$(Ba_{0.75}Sr_{0.25})Ti_{1.006}O_{3.012}$ + 1.2 wt.% La_2O_3 + 1.0 wt.% Sb_2O_3
B4	0.006	1.6	$(Ba_{0.75}Sr_{0.25})Ti_{1.006}O_{3.012}$ + 1.6 wt.% La_2O_3 + 1.0 wt.% Sb_2O_3

3. Results and discussion

3.1. XRD and SEM analysis

The X-ray diffraction patterns of as sintered La_2O_3 doped $(Ba_{0.75}Sr_{0.25})Ti_{1+\delta}O_{3+2\delta}$ bulk ceramics are shown in Fig. 1. As indicated in Fig. 1a, all these polycrystals are single-phase solid solutions with a typical perovskite structure, which implies that La^{3+} ions have been incorporated into the lattice of the non-stoichiometric barium strontium titanate solid solution. The XRD profiles focusing on the (1 1 0) diffraction peaks of the BST samples with different non-stoichiometric levels (namely δ) and La_2O_3 doping concentrations (namely x) are presented in Fig. 1b and Fig. 1c, respectively. With the increase of δ, a slight shift of diffraction peaks for the perovskite phase to lower two-theta values is observed (Fig. 1b), which indicates that the unit cell volumes of ABO_3 perovskite lattices increase as the δ increases. Also, the lattice parameters a and c of the tetragonal cell as well as the unit cell volumes, shown in Fig. 2, are calculated according to the peak locations and Miller indices. It can be seen that the unit cell volumes of perovskite lattice increase as the δ increases.

Fig. 1c shows that the diffraction peaks move towards lower two-theta values and then shift to higher two-theta values as the La_2O_3 doping content increases in $(Ba_{0.75}Sr_{0.25})Ti_{1.006}O_{3.012}$ ceramics, which reveals a variation of the unit cell volume of the La_2O_3 doped Ti-rich BST ceramics. Fig. 3 shows the lattice parameters a and c of the tetragonal cell as well as the unit cell volume as a function of La_2O_3 content. It is found that with the increase of La_2O_3 addition content, the unit cell volume increases and then decreases slightly.

It is believed that A-site vacancies V''_A and oxygen vacancies $V_{\ddot{O}}$, which are revealed by the following point defect reaction equation:

$$(Ba_{0.75}Sr_{0.25})Ti_{1+\delta}O_{3+2\delta} \rightarrow 0.75Ba_{Ba} + 0.25Sr_{Sr} + (1+\delta)Ti_{Ti} + (3+2\delta)O_O + \delta V''_A + \delta V_{\ddot{O}} \quad (4)$$

may appear in the Ti-rich $(Ba_{0.75}Sr_{0.25})Ti_{1+\delta}O_{3+2\delta}$ ceramics. Therefore, the concentration of V''_A and $V_{\ddot{O}}$ vacancies increases with the increasing δ value. As reported previously, with increasing Sb_2O_3 concentration in Ti-rich BST ceramics, Sb^{3+} ions initially enter the A-site vacancies V''_A to diminish the V''_A concentration and then partially substitute for the A-site ions in perovskite lattice to generate more A-site vacancies V_A'' [17]. So, in the considered 1.0 wt.% Sb_2O_3 doped $(Ba_{0.75}Sr_{0.25})Ti_{1+\delta}O_{3+2\delta}$ ceramics, the larger the δ value, the more Sb^{3+} ions are needed to neutralize the A-site vacancies V''_A shown in equation 4 and less remaining Sb^{3+} ion can contribute to the generation of new V''_A, which means that the larger the δ value, the less V''_A vacancies remain in the present $(Ba_{0.75}Sr_{0.25})Ti_{1+\delta}O_{3+2\delta}$ ceramics. It is exactly the decreasing V''_A concentration that makes the unit cell volume increasing with the increase of δ value.

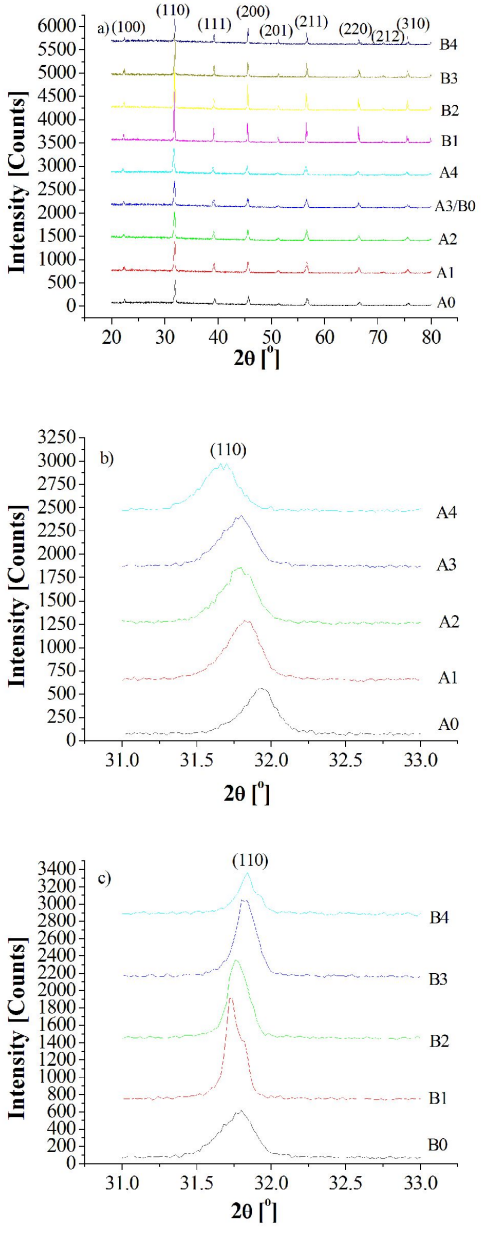

Fig. 1. XRD patterns of La_2O_3 doped $(Ba_{0.75}Sr_{0.25})Ti_{1+\delta}O_{3+2\delta}$ ceramics, (a) for all studied samples; profiles focusing on (1 1 0) diffraction peaks for (b) samples with different δ; (c) samples with different x.

With lanthanide contraction, the site occupation of rare earth ions in $BaTiO_3$ changes as follows: Ba sites → both Ba and Ti sites → Ti sites [18]. It is believed that La^{3+} ions commonly enter the A sites of BT [19] and BST perovskite structure [14].

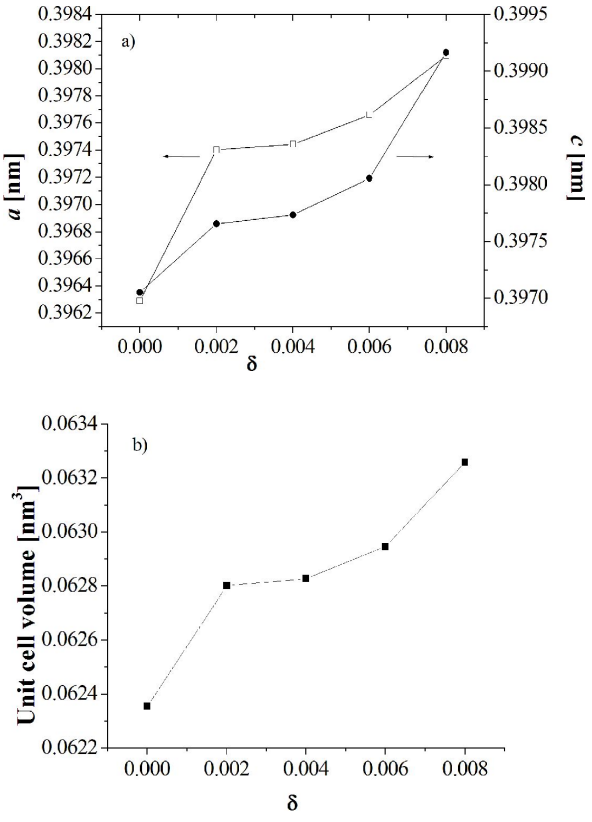

Fig. 2. The lattice parameters and unit cell volumes of $(Ba_{0.75}Sr_{0.25})Ti_{1+\delta}O_{3+2\delta}$ samples as a function of non-stoichiometric level δ.

Since the equation 4 is valid and A-site vacancies V''_A exist in the $(Ba_{0.75}Sr_{0.25})Ti_{1+\delta}O_{3+2\delta}$ ceramics, after doping La_2O_3, La^{3+} ions gradually enter the A-sites in perovskite lattice to fill in the A-site vacancies V''_A. Until the A-site vacancies V''_A are neutralized by La^{3+} ions, A-site ions in the perovskite lattice start to be partially occupied by La^{3+} ions. Then the following defect reaction takes place:

$$La_2O_3 \rightarrow 2La_A^{\cdot} + V_A'' + 3O_O \qquad (5)$$

Therefore, the V''_A concentration decreases first and then increases with the increasing La_2O_3 doping content and correspondingly the unit cell volume increases and then decreases with the increase of La_2O_3 content. In terms of size, the ionic radii of $Ba^{2+}$and Sr^{2+} in 12 coordination are 0.161 nm and 0.144 nm, respectively. The radius of La^{3+} ion in 12 coordination is 0.132 nm which is smaller than that of A-site ions. When La^{3+} ions substitute

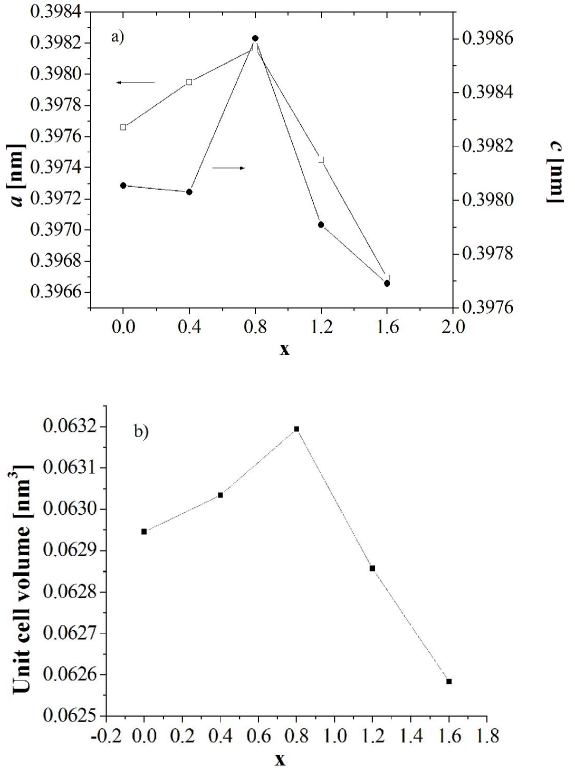

Fig. 3. The lattice parameters and unit cell volumes of $(Ba_{0.75}Sr_{0.25})Ti_{1+\delta}O_{3+2\delta}$ samples as a function of La_2O_3 content x.

the host A-site ions, the unit cell volume decreases with increasing La_2O_3 content due to the smaller ionic size of La^{3+}. For $(Ba_{0.75}Sr_{0.25})Ti_{1+\delta}O_{3+2\delta}$ samples with high La_2O_3 content, both the increasing V''_A concentration and the smaller ionic radius of La^{3+} contribute to the decrease of the unit cell volume.

Fig. 4 shows the surface morphologies of La_2O_3 doped Ti-rich $(Ba_{0.75}Sr_{0.25})Ti_{1.006}O_{3.012}$ ceramics. It appears that all the samples exhibit dense microstructure and no abnormal grain growth is observed. There is no obvious change in the average grain size between the 0.4 wt.% La_2O_3 doped $(Ba_{0.75}Sr_{0.25})Ti_{1.006}O_{3.012}$ ceramics and the 0.8 wt.% La_2O_3 doped ones, showing that the low La_2O_3 addition level makes little contribution to refining the grain size. However, the distinctly decreased average grain size and fine grain size distribution can be obtained in 1.6 wt.% La_2O_3 doped $(Ba_{0.75}Sr_{0.25})Ti_{1.006}O_{3.012}$ ceramics.

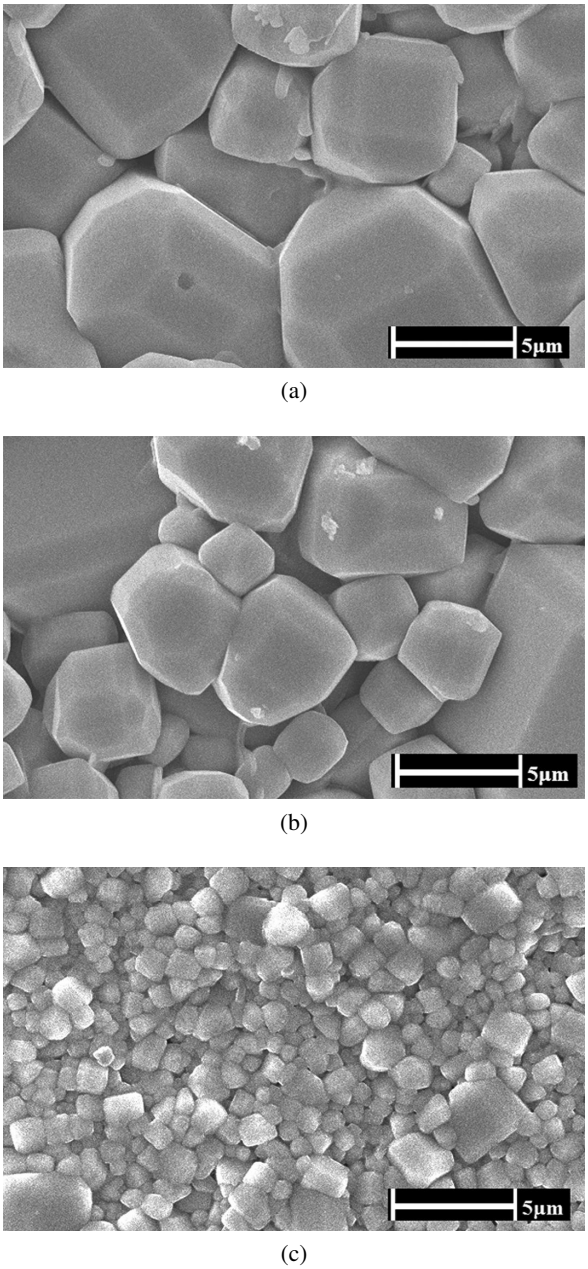

Fig. 4. SEM micrographs of La_2O_3 doped $(Ba_{0.75}Sr_{0.25})Ti_{1.006}O_{3.012}$ ceramics: (a) $La_2O_3 = 0.4$ wt.%; (b) $La_2O_3 = 0.8$ wt.%; (c) $La_2O_3 = 1.6$ wt.%.

The surface morphologies of $(Ba_{0.75}Sr_{0.25})Ti_{1+\delta}O_{3+2\delta}$ ceramics are shown in Fig. 5. The refinement of the grain size distribution is observed with the increasing non-stoichiometric level δ. In addition, the average grain size of $(Ba_{0.75}Sr_{0.25})Ti_{1.008}O_{3.016}$

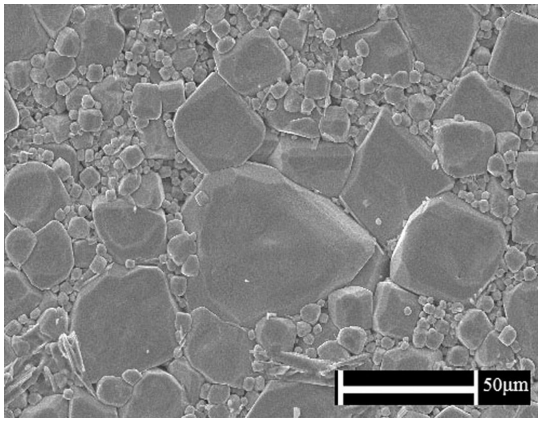

(a)

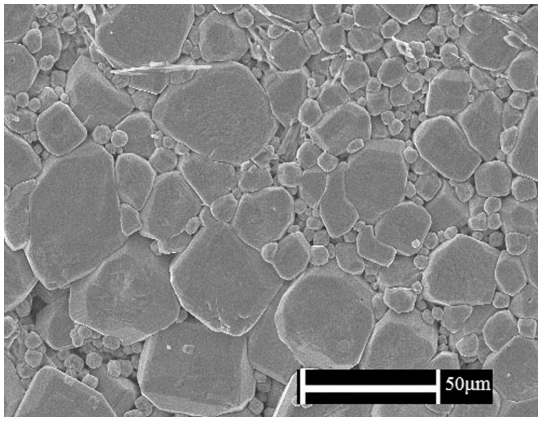

(b)

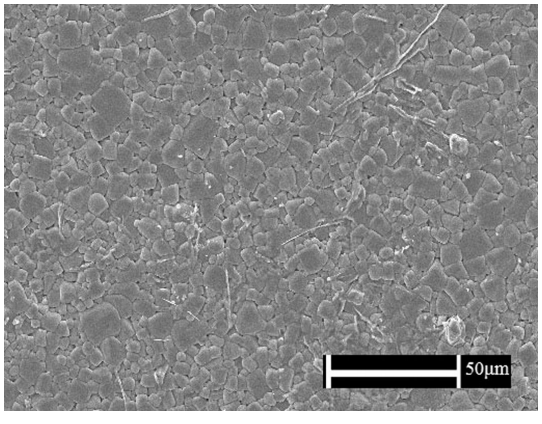

(c)

Fig. 5. SEM micrographs of $(Ba_{0.75}Sr_{0.25})Ti_{1+\delta}O_{3+2\delta}$ ceramics: (a) $\delta = 0.002$; (b) $\delta = 0.004$; (c) $\delta = 0.008$.

($\delta = 0.008$) ceramics is much smaller than that of $(Ba_{0.75}Sr_{0.25})Ti_{1.002}O_{3.004}$ ($\delta = 0.002$) and $(Ba_{0.75}Sr_{0.25})Ti_{1.004}O_{3.008}$($\delta = 0.004$) ceramics.

3.2. Dielectric characteristics

Table 2 shows the relative dielectric constant and dielectric loss of $(Ba_{0.75}Sr_{0.25})Ti_{1+\delta}O_{3+2\delta}$ ceramics as a function of non-stoichiometric level δ at room temperature. It is obvious that all the non-stoichiometric $(Ba_{0.75}Sr_{0.25})Ti_{1+\delta}O_{3+2\delta}$ ceramics possess high relative dielectric constant which is more than 3500 at room temperature. The relative dielectric constant and dielectric loss decrease and then increase with the increasing δ value.

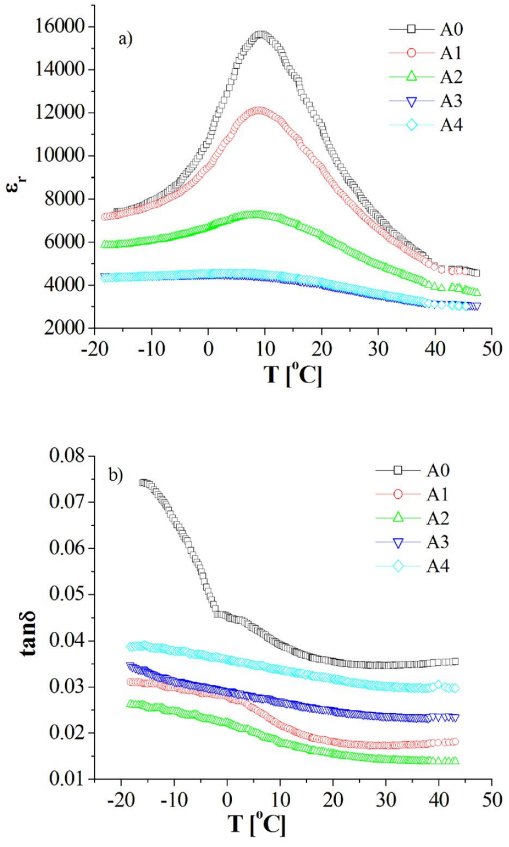

Fig. 6. Temperature dependence of (a) relative dielectric constant and (b) dielectric loss for $(Ba_{0.75}Sr_{0.25})Ti_{1+\delta}O_{3+2\delta}$ ceramics.

Temperature dependence of the relative dielectric constant and dielectric loss for the $(Ba_{0.75}Sr_{0.25})Ti_{1+\delta}O_{3+2\delta}$ ceramics is shown in Fig. 6. The relative dielectric constant first increases, achieves a maximum (ϵ_{rmax}) and then decreases with increasing temperature. As shown

Table 2. Dielectric parameters for $(Ba_{0.75}Sr_{0.25})Ti_{1+\delta}O_{3+2\delta}$ ceramics.

δ	ϵ_{rRT}	$\tan\delta_{RT}$	ϵ_{rmax}	ΔC/C (−20 °C to 45 °C) [%]	TCC [ppm/°C]
0.000	8760	0.0348	15644	−46.3 to +78.6	−60270 to +3819
0.002	7803	0.0174	12101	−40.6 to +55.1	−46091 to +1897
0.004	5539	0.0146	7258	−31.9 to +31.0	−38775 to 0
0.006	3788	0.0242	4505	−18.6 to +18.9	−16621 to 0
0.008	3848	0.0307	4551	−21.2 to +18.3	−17325 to 0

in Table 2, the relative dielectric constant maximum decreases significantly and then increases slightly with the increasing δ value. Also, it is noteworthy that in the whole temperature range the higher the δ value, the lower the relative dielectric constant of $(Ba_{0.75}Sr_{0.25})Ti_{1+\delta}O_{3+2\delta}$ ceramics. The diffused phase transition is visible in $(Ba_{0.75}Sr_{0.25})Ti_{1+\delta}O_{3+2\delta}$ ceramics with high δ value. The percentage of capacitance variation (ΔC/C) and the temperature coefficient of capacitance (TCC) used for accessing the temperature stability of relative dielectric constant are calculated according to equation 6 and equation 7:

$$\Delta C/C = \frac{C_t - C_{RT}}{C_{RT} \times 100\ \%} \tag{6}$$

$$TCC = \frac{C_t - C_{RT}}{C_{RT}(T_t - 25)} \tag{7}$$

where C_{RT} is the capacitance value at room temperature (namely 25 °C); C_t is the capacitance value at any other temperature. As shown in Table 2, the percentage of capacitance variation decreases with the increase of δ value, which indicates that Ti-rich $(Ba_{0.75}Sr_{0.25})Ti_{1+\delta}O_{3+2\delta}$ ceramics with high non-stoichiometric level are promising for the temperature stable capacitor applications. In other words, the temperature stability of relative dielectric constant for $(Ba_{0.75}Sr_{0.25})Ti_{1+\delta}O_{3+2\delta}$ ceramics can be improved by increasing δ, which can be explained using the so called grain boundary effect. The diffusion of non-ferroelectric grain boundaries among the barium strontium titanate ferroelectric grains helps the orientation of ferroelectric domains below the Curie temperature, which makes the ferroelectric-paraelectric phase transition possible in a relative broad temperature range. The average grain size of $(Ba_{0.75}Sr_{0.25})Ti_{1+\delta}O_{3+2\delta}$ ceramics with high non-stoichiometric level is reduced obviously compared with the low non-stoichiometric level samples, which means the grain boundary buffering effect becomes more significant in high non-stoichiometric level samples. Macroscopically, the Curie peak for high δ samples is broader than that for low δ ones, as shown in Fig. 6a. It was reported that the lattice deformation and inner stresses can cause the increase in relative dielectric constant [20]. The decreasing V''_A concentration resulting in the expansion of unit cell volume with the increase of δ value, as mentioned above, makes the lattice deformation and inner stress in $(Ba_{0.75}Sr_{0.25})Ti_{1+\delta}O_{3+2\delta}$ ceramics released, which explains the decrease of ϵ_{rRT} and ϵ_{rmax} with the increasing δ value in present $(Ba_{0.75}Sr_{0.25})Ti_{1+\delta}O_{3+2\delta}$ ceramics. As shown in Fig. 6b, the non-stoichiometric $(Ba_{0.75}Sr_{0.25})Ti_{1+\delta}O_{3+2\delta}$ ceramics exhibits lower dielectric loss than that of stoichiometric $(Ba_{0.75}Sr_{0.25})TiO_3$ ceramics in the studied temperature range.

Above the ferroelectric- paraelectric transition temperature, the relative dielectric constant of ferroelectrics as a function of temperature can be described by the Curie-Weiss law:

$$\varepsilon_r = \frac{k}{T - T_0} \tag{8}$$

where k is the Curie constant and T_0 is the Curie-Weiss temperature. Therefore, the temperature dependence of inverse dielectric constant $1/\epsilon_r$ can be expressed linearly:

$$1/\varepsilon_r = \frac{1}{k} \cdot T - \frac{T_0}{k} \tag{9}$$

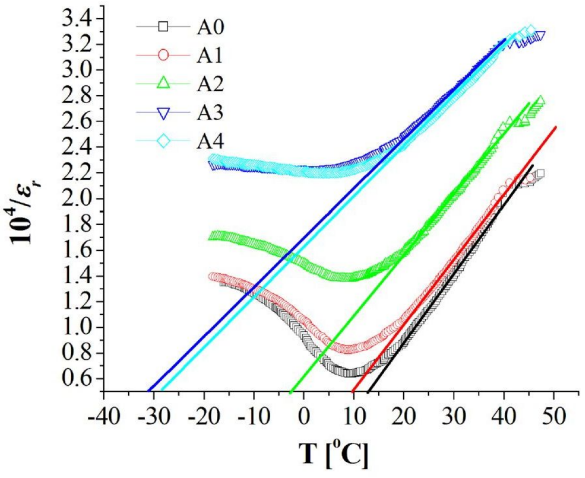

Fig. 7. Temperature dependence of inverse dielectric constant for $(Ba_{0.75}Sr_{0.25})Ti_{1+\delta}O_{3+2\delta}$ ceramics.

The temperature dependence of inverse dielectric constant for $(Ba_{0.75}Sr_{0.25})Ti_{1+\delta}O_{3+2\delta}$ ceramics is shown in Fig. 7. The Curie-Weiss temperature and Curie transition temperature for $(Ba_{0.75}Sr_{0.25})Ti_{1+\delta}O_{3+2\delta}$ ceramics are shown in Table 3. With an increase in δ, there is no obvious shift for Curie temperature which is constant at about 9 °C for all $(Ba_{0.75}Sr_{0.25})Ti_{1+\delta}O_{3+2\delta}$ samples. A large difference between the Curie-Weiss temperature and Curie temperature of $(Ba_{0.75}Sr_{0.25})Ti_{1+\delta}O_{3+2\delta}$ samples with high non-stoichiometric level can be noticed.

Table 3. Characteristic constants of the ferroelectric transition for $(Ba_{0.75}Sr_{0.25})Ti_{1+\delta}O_{3+2\delta}$ ceramics.

δ	T_c [°C]	T_{c-w} [°C]
0.000	9.3	13
0.002	9.1	10
0.004	9.2	−3
0.006	8.9	−31
0.008	8.6	−28

Table 4 shows the relative dielectric constant, dielectric loss and resistivity of La_2O_3 doped $(Ba_{0.75}Sr_{0.25})Ti_{1.006}O_{3.012}$ ceramics as a function of La_2O_3 content at room temperature. With the increase of La_2O_3 doping content, the relative dielectric constant and resistivity increase initially and then decrease. The 1.2 wt.% La_2O_3 doped sample still has a high relative dielectric constant which is more than 3500. The dielectric loss decreases with the increasing La_2O_3 content.

Table 4. Dielectric parameters for La_2O_3 doped $(Ba_{0.75}Sr_{0.25})Ti_{1.006}O_{3.012}$ ceramics.

x	ϵ_{rRT}	$\tan\delta_{RT}$	ρ_{RT} [10^4 Ω·m]
0	3788	0.0242	2.25
0.4	5381	0.0236	2.70
0.8	4002	0.0217	4.24
1.2	3772	0.0125	1.60
1.6	2612	0.0103	0.97

Temperature dependence of the relative dielectric constant and dielectric loss for La_2O_3 doped $(Ba_{0.75}Sr_{0.25})Ti_{1.006}O_{3.012}$ ceramics is shown in Fig. 8. The Curie temperature of 0 wt.% La_2O_3 doped $(Ba_{0.75}Sr_{0.25})Ti_{1.006}O_{3.012}$ ceramics is above 0 °C as mentioned previously. The Curie temperature of 0.4 wt.% La_2O_3 doped $(Ba_{0.75}Sr_{0.25})Ti_{1.006}O_{3.012}$ ceramic is −3.6 °C while those of the samples with high La_2O_3 content are below −18 °C, which falls out of the studied temperatures range. The maximum relative dielectric constant ϵ_{rmax} of 0 wt.% La_2O_3 doped sample is 4505 as shown in Table 2 while that of 0.4 wt.% La_2O_3 doped sample is around 15972. The ϵ_{rmax} of 0.8 wt.% La_2O_3 doped sample is higher than 17500, which implies that low La_2O_3 doping content can enhance the permittivity maximum value. Similar phenomenon has been reported for $BaTiO_3$ ceramics. For the composition $Ba_{1-x}La_xTi_{1-x/4}O_3$, where x = 0.05, the permittivity has a maximum value of 19000 at 18 °C, compared with a typical value of 10000 at 130 °C in undoped $BaTiO_3$ ceramics [21]. The value of permittivity maximum at the tetragonal/cubic phase transition in ceramic samples prepared in O_2 increased to ∼25 000 for x = 0.06 at −9 °C [22].

With increasing La_2O_3 doping content, the decreased V''_A concentration and correspondingly

the increased unit cell volume lead to a longer distance between the central ion and its nearest neighbors in the oxygen octahedron in perovskite lattice as well as the decreased inner stresses. The movement of the central ion is relatively less confined, which enhances the spontaneous polarization of the perovskite grain lattice and results in increasing ϵ_{rmax} for low La_2O_3 content doped non-stoichiometric BST ceramics. However, the decreased inner stresses which make the ϵ_{rmax} decreasing become competitive against the increased spontaneous polarization. Apparently, the increased spontaneous polarization is the predominant factor for La_2O_3 doped samples between the conflicting two since the ϵ_{rmax} increases with the increasing La_2O_3 content. When La^{3+}ions substitute the host A-site ions in high La_2O_3 content samples, such as B4, the weakened spontaneous polarization, which is attributed to the decreased unit cell volume and thus the decreased ϵ_{rmax}, can be predicted.

As shown in Fig. 8, the flattened curves of relative dielectric constant as a function of temperature for the 0 wt.% and 1.6 wt.% La_2O_3 doped $(Ba_{0.75}Sr_{0.25})Ti_{1.006}O_{3.012}$ ceramics indicate an improved temperature stability compared with the low doping content samples such as B1, B2 and B3. The decreased average grain size and fine grain size distribution in high La_2O_3 content samples, as shown in Fig. 4c, contribute to the improvement of relative dielectric constant temperature stability.

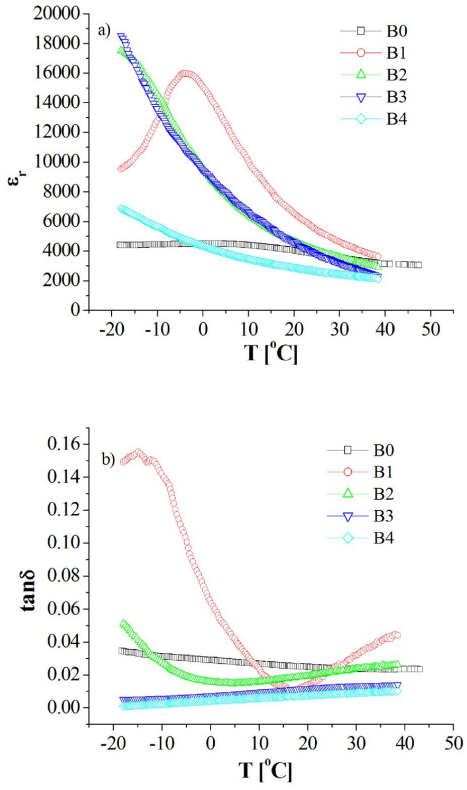

Fig. 8. Temperature dependence of relative dielectric constant and dielectric loss for La_2O_3 doped $(Ba_{0.75}Sr_{0.25})Ti_{1.006}O_{3.012}$ ceramics.

4. Conclusions

The La_2O_3 doped Ti rich barium strontium titanate ceramic samples for capacitor applications were prepared by conventional solid state method. Their microstructures and dielectric properties were investigated with non-stoichiometric level and various La_2O_3 content by SEM, XRD and LCR measuring system. It is revealed that:

1. 0 wt.% to 1.6 wt.% La_2O_3 doped $(Ba_{0.75}Sr_{0.25})Ti_{1+\delta}O_{3+2\delta}$ ($\delta = 0$ to 0.008) bulk ceramics are single-phase solid solutions with a typical perovskite structure. The unit cell volumes of Ti-rich barium strontium titanate perovskite lattice increase with the increase of non-stoichiometric level. With the increasing La_2O_3 content, the unit cell volume increases and then decreases slightly owing to the variation of V''_A concentration and the difference of ionic radii between La^{3+} ions and A-site host ions.
2. The average grain size and grain size distribution of Ti-rich barium strontium titanate ceramics can be refined by using relatively high non-stoichiometric level and high La_2O_3 content.
3. The relative dielectric constant and dielectric loss at room temperature as well as the relative dielectric constant maximum decrease and then increase with the increasing non-stoichiometric level. Also,

the temperature stability of the relative dielectric constant for Ti-rich barium strontium titanate ceramics can be improved by increasing non-stoichiometric level due to the grain boundary buffering effect.

4. With the increase of La_2O_3 doping content, the relative dielectric constant at room temperature increases initially and then decreases. However, the dielectric loss decreases with the increasing La_2O_3 content. The relative dielectric constant maximum is enhanced due to the increased spontaneous polarization in Ti-rich barium strontium titanate ceramics with low La_2O_3 content.

Acknowledgements

This work is sponsored by the Suzhou Pante Electric Ceramics Tech. Co. Ltd. This work is also supported by the Natural Science Foundation of Jiangsu Province in China (BK20140517) and the University Natural Science Project of Jiangsu Province in China (14KJB430011).

References

[1] MEGAW H.D., *Nature*, 155 (1945), 484.
[2] HAN H., VOISIN C., FRITSCH S.G., DUFOUR P., TENAILLEAU C., TURNER C., NINO J.C., *J. Appl. Phys.*, 113 (2013), 024102.
[3] HAN H., GHOSH D., JONES J.L., NINO J.C., *J. Am. Ceram. Soc.*, 96 (2013), 485.
[4] JIAN G., ZHOU D., YANG J., SHAO H., XUE F., FU Q., *J. Eur. Ceram. Soc.*, 33 (2013), 1155.
[5] KAY H.F., VOUSDEN P., *Philos. Mag.*, 40 (1949), 1019.
[6] CAO W.Q., XU L.F., ISMAIL M.M., HUANG L.L., *Mater. Sci.-Poland*, 34 (2016), 322.
[7] WEI X., YAO X., *Mater. Sci. Eng. B-Adv.*, 99 (2003), 74.
[8] ZHANG L.H., WANG S.L., LIU F.H., *J. Electron. Mater.*, 44 (2015), 3408.
[9] DONG H., JIN D., XIE C., CHENG J., ZHOU L., CHEN J., *Mater. Lett.*, 135 (2014), 83.
[10] LI Y., QU Y., *Mater. Res. Bull.*, 44 (2009), 82.
[11] PAHUJA P., KOTNALA R.K., TANDON R.P., *J. Alloy Compd.*, 617 (2014), 140.
[12] HERNER S.B., SELMI F.A., VARADAN V.V., VARADAN V.K., *Mater. Lett.*, 15 (1993), 317.
[13] LIANG X., MENG Z., WU W., *J. Am. Ceram. Soc.*, 87 (2004), 2218.
[14] ZHANG J., ZHAI J., CHOU X., YAO X., *Mater. Chem. Phys.*, 111 (2008), 409.
[15] ZHANG C., QU Y., *T. Nonferr. Metal. Soc.*, 22 (2012), 2742.
[16] KISHI H., MIZUNO Y., CHAZONO H.,*Jpn. J. Appl. Phys.*, 42 (2003), 1.
[17] ZHANG C., LING Z., JIAN G., *J. Mater. Sci.-Mater. El.*, 27 (2016), 11770.
[18] LU D.Y., SUN X.Y., TODA M., *J. Phys. Chem. Solids*, 68 (2007), 650.
[19] TSUR Y., DUNBAR T.D., RANDALL C.A., *J. Electroceram.*, 7 (2001), 25.
[20] LI W., QI J., WANG Y., LI L., GUI Z., *Mater. Lett.*, 57 (2002), 1.
[21] MORRISON F.D., SINCLAIR D.C., SKAKLE J.M.S., WEST A.R., *J. Am. Ceram. Soc.*, 81 (1998), 1957.
[22] MORRISON F.D., SINCLAIR D.C., WEST A.R., *J. App. Phys.*, 86 (1999), 6355.

Received 2017-03-20
Accepted 2017-11-29